Journal of Molecular Structure 1037 (2013) 130–135

Contents lists available at SciVerse ScienceDirect

Journal of Molecular Structure

journal homepage: www.elsevier.com/locate/molstruc

Self-assemblies, helical ribbons and gelation tuned by solvent–gelator interaction in a bi-1,3,4-oxadiazole gelator

Chengxiao Zhao [a], Binglian Bai [b], Haitao Wang [a], Songnan Qu [c], Guanjun Xiao [d], Taiji Tian [a], Min Li [a,*]

[a] Key Laboratory of Automobile Materials, Ministry of Education, Institute of Materials Science and Engineering, Jilin University, Changchun 130012, PR China
[b] College of Physics, Jilin University, Changchun 130012, PR China
[c] Key Laboratory of Excited State Processes, Changchun Institute of Optics, Fine Mechanics and Physics, Chinese Academy of Sciences, Changchun 130033, PR China
[d] State Key Laboratory of Superhard Materials, Jilin University, Changchun 130012, PR China

HIGHLIGHTS

- H-aggregate and slipped aggregate of BOXDH-T12 could be obtained by controlling hydrogen bonding formation.
- Helical fibers of BOXDH-T12 could be obtained by adding ethanol into DMSO solution.
- It was demonstrated that the solvophobic/solvophilic effect played a critical role in alcohol gels.

GRAPHICAL ABSTRACT

FTIR, ^{1}H NMR, WAXD and TGA results suggested that strong gelator–gelator intermolecular hydrogen bonding interaction induced H-aggregation of BOXDH-T12 while the interaction between DMSO and BOXDH-T12 molecules caused the slipped stacking. Adding ethanol into DMSO solution of BOXDH-T12, morphologies changed from microparticles to helix.

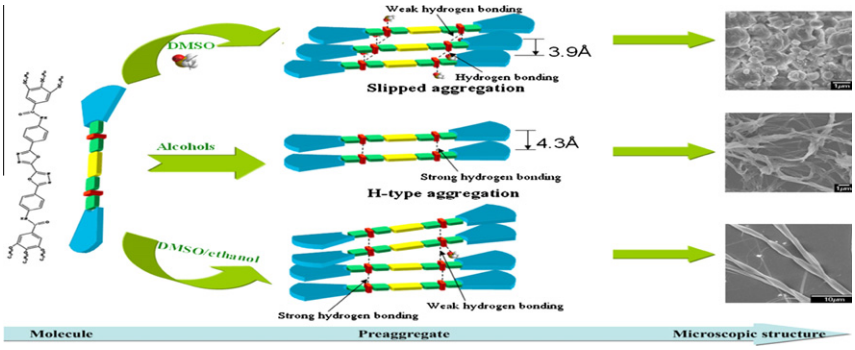

ARTICLE INFO

Article history:
Received 26 October 2012
Received in revised form 11 December 2012
Accepted 13 December 2012
Available online 2 January 2013

Keywords:
Bi-1,3,4-oxadiazole
H-aggregation
Hydrogen bond
Organogel
Helical fiber

ABSTRACT

A bi-1,3,4-oxadiazole derivative (BOXDH-T12) showed intramolecular charge transition at concentrations lower than 1×10^{-5} mol/L. The self-assembling behaviors of BOXDH-T12 depended on solvents that it self-assembled into H-aggregates in alcohols and slipped packing aggregates in DMSO. FTIR, ^{1}H NMR and TGA results revealed that strong gelator–gelator hydrogen bonding interaction induced H-aggregation of BOXDH-T12 in alcohols and the interactions between DMSO and BOXDH-T12 molecules caused a slipped stacking. BOXDH-T12 can gel the mixtures of DMSO and ethanol through a cooperative effect of the hydrogen bonding, van der Waals interaction and π–π stacking forces, furthermore, helical ribbons could be observed in DMSO/ethanol due to DMSO molecule interacting. In alcohols, solvophobic/solvophilic effect plays a critical role in gelation behaviors.

1. Introduction

Self-assembled materials are of special interest since their aggregate structures and their properties can be steered in a wide range [1]. For instance, self-assembly of small molecular entities into well-defined supramolecular architectures is involved in electron-transporting materials [2] and in various vital biological functions in living systems [3]. For a rational design of supramolecular functionalities, detailed knowledge of the effects determining the self-assembly process and the optical properties is required. Over the past decade, noncovalent interactions such as hydrogen

* Corresponding author.
E-mail address: minli@jlu.edu.cn (M. Li).

0022-2860/$ - see front matter © 2012 Elsevier B.V. All rights reserved.
http://dx.doi.org/10.1016/j.molstruc.2012.12.037

bonding, metal-ion-to-ligand coordination, electrostatic interactions, π–π stacking, dipole–dipole interactions, and hydrophobic interactions, have been identified as enabling the construction of various superstructures from specifically engineered small molecule building blocks [4]. π-conjugated molecules could provide highly ordered organized structures through π–π stacking interactions and hydrogen-bonding [4,5]. The directional force such as hydrogen bonding can control the strength of the interactions between the π-planes; as a result, the balance between hydrogen bonding and the π–π stacking would tune the electronic and electrooptical properties and the structures of molecular assemblies in soft materials. For example, Würthner and co-workers obtained J-aggregates of PBI by encoding in the molecular building block [6], whereas Maeda [7] and Bo [8] obtained H-aggregates by introducing amide groups in gelator molecules. Yagai reported the transformation from H- to J-aggregated PBI through hydrogen-bond-directed complexation between melamine and cyanurate [9]. In some case, the directional forces would cause a gel formation and are significantly influenced by various conditions including the solvents [7,10]. For a specific gelator, especially the hydrogen bonding gelator, the forces could be influenced by solvent–gelator interactions. For example, Dey demonstrated the gelation of N-(n-alkylcarbamoyl)-L-alanine could be tuned by turning the intermolecular H-bonding interaction by adding a small amount of water or methanol [11]. Park reported a nonfluorescent benzene-1,3,5-tricarboxamide derivative (TOBA) with three 2,5-diphenyl [1,3,4] oxadiazole arms, which could gel some aprotic organic solvents and exhibited the enhanced fluorescence emission in gels due to the face-to face intermolecular H-bonding interaction [12].

On the other hand, the self-aggregate morphologies could be tuned by changing environments, such as cooling rate, proportion of binary solvents, additive. Weiss et al. obtained different length and thickness fibers of anthraquinone-appended steroid-based gelators by controlling the cooling rate [13]. Wan and coworkers observed helical ribbons of 4″-butoxy-4-hydroxy-*p*-terphenyl-*β*-D-glucoside (BHTG) in1,4-dioxane and the mixture of 1,4-dioxane and water, and the handedness depended on the rate of gel formation [14]. In related work, Li reported the structural transition of an organogel self-assembled form a single dipeptide building block, diphenylalanine (L-Phe-L-Phe, FF), in toluene into a flower-like microcrystal merely by introducing ethanol as a co-solvent [15].

Previously, we reported the synthesis and self-assembly behaviors of 1,3,4-oxadiazole derivatives and the results showed that J-aggregates and supramolecular gels of 2,2′-bis(3,4,5-trioctanoxyphenyl)-bi-1,3,4-oxadiazole (BOXD-T8) formed in ethanol and DMSO through the interactions between rod-like π-planes as well as van der Waals interactions of long alkyl chains [16]. We expected that the introduction of additional hydrogen-bonding sites such as amide moieties might influence the supramolecular assemblies. In this study, we report the self-assembly of an amide-containing bi-1,3,4-oxadiazole derivative (BOXDH-T12, Scheme 1) [17] in different solvents and the effect of solvents on its gelation behavior. Our results indicated that BOXDH-T12 self-assembled

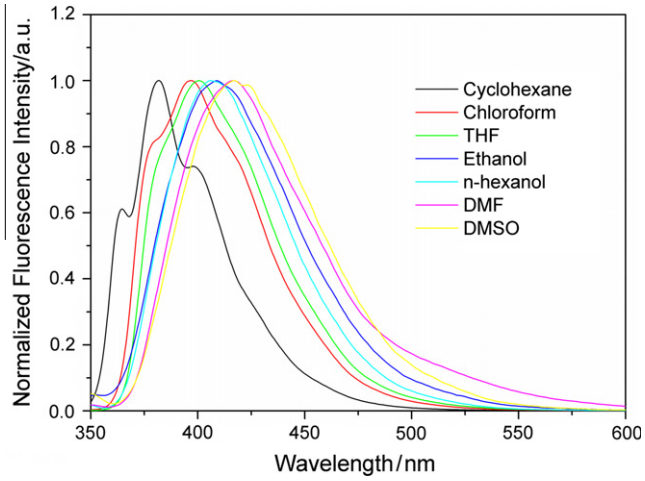

Fig. 1. Normalized fluorescence spectra of BOXDH-T12 in different solvents at concentration of 1×10^{-5} mol/L.

Table 1
Photophysical properties of BOXDH-T12 in different solvents (1×10^{-5} mol/L).

Solvent	λ_{abs} (nm)	λ_{em} (nm)	Stokes shift (cm^{-1})	Φ_F
DMSO[a]	337	419	5807	0.09
DMF	338	417	5605	0.03
Ethanol[a]	333	409	5224	0.14
n-hexanol[a]	339	410	5108	0.25
THF	337	381, 401, 420	4736	0.3
Chloroform	337	379, 397, 417	4484	0.51
Cyclohexane[a]	328	364, 381, 401	4241	0.56

[a] BOXDH-T12 in these solvents were measured at 60 °C.

to H-aggregates in alcohols and slipped stacking aggregates in DMSO. Alcohols with long chains and mixtures of DMSO and ethanol could be gelled by BOXDH-T12 while precipitates in ethanol and n-propanol. BOXDH-T12 gel these solvents through a cooperative effect of the hydrogen bonding, van der Waals interactions, π–π stacking force and solvophobic/solvophilic effect.

2. Results and discussion

2.1. Solvent-polarity-dependent PL

The optical properties of BOXDH-T12 in various solvents (1×10^{-5} mol/L) are shown in Fig. 1 and Table 1. BOXDH-T12 exhibited strong fluorescence ($\Phi = 0.56$) with vibronic structure in cyclohexane. The emission maximum red-shifted from 381 nm (in cyclohexane) to 419 nm (in DMSO) with an increase of the solvent polarity, meanwhile, the fluorescence quantum yield decreased from 0.56 (in cyclohexane) to 0.09 (in DMSO), and no vibronic structures were observed in polar solvents. In the concentration-dependent emission spectra (Fig. S1), both the shapes and the maximum of the emissions remained unchanged, moreover,

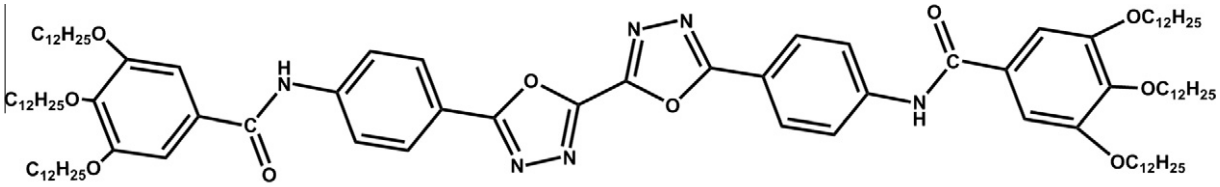

BOXDH-T12

Scheme 1. Molecular structure of the gelator BOXDH-T12.

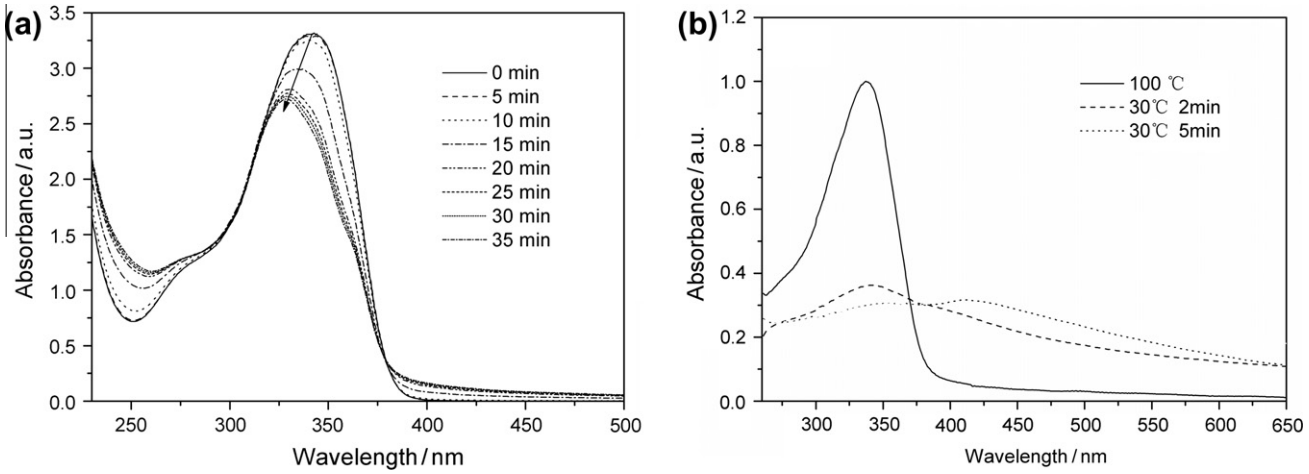

Fig. 2. UV–vis spectra of BOXDH-T12 in (a) n-hexanol (5.0×10^{-4} mol/L) and (b) DMSO solutions (2.9×10^{-4} mol/L) in 1 mm cell measured by heating to isotropic solution and holding at 6 °C and 30 °C, respectively, for different time period.

the intensity of the emissions was nearly proportional to the concentrations within the range of 10^{-5}–10^{-7} mol/L, indicating its monomeric feature. Thus, observations of the red-shifted and decreased fluorescence emission and the unresolved vibronic structure in the photoluminescence (PL) spectra in polar solvents suggested the formation of intramolecular charge transitions [18].

2.2. Solvent-dependent self-assembly

BOXDH-T12 with additional hydrogen-bonding sites (amide groups) may interact with the hydrogen bonding acceptor (HBA) or hydrogen bonding donor (HBD) solvents through hydrogen bonding, which may further influence the self-assembly of BOXDH-T12. Thus, we investigated its self-assembly in alcohols and DMSO, whose self-assembly processes were envisioned by the changes of the UV–vis absorption and Fluorescence emission. The UV–vis spectra of BOXDH-T12 in n-hexanol (5.0×10^{-4} mol/L) and DMSO solutions (2.9×10^{-4} mol/L) were shown in Fig. 2. Blue-shifted UV–vis absorption and weakened Fluorescence emission of BOXDH-T12 in n-hexanol were observed during storage at 6 °C for 35 min (gel formation) as shown in Figs. 2a and S2a. The main absorption peak at 341 nm decreased and blue-shifted to 328 nm (Fig. 2a), and the Fluorescence emission weakened dramatically (Fig. S2a), indicating the characteristic H-type aggregation [19]. A similar H-type self-assembly behavior was also demonstrated in the other alcohols, such as ethanol and n-octanol, due to the blue-shifted absorption (Fig. S3). In contrast, red-shifted absorption and intensified Fluorescence emission of BOXDH-T12 were observed in DMSO. As given in Fig. 2b, the main absorption peak at 337 nm decreased and red-shifted to 345 nm, meanwhile a new shoulder band at 420 nm intensified during storage at 30 °C for 5 min. Moreover, the Fluorescence emission of BOXDH-T12 in DMSO intensified and slightly red-shifted (ca. 5 nm) (Fig. S2b), which implies that more slipped aggregates of BOXDH-T12 formed in DMSO. XRD pattern of the xerogel from n-hexanol shows five diffraction peaks corresponding to *d*-spacing of 42.2, 13.2, 8.4, 6.1 and 4.3 Å (Fig. 3a), and the precipitate from DMSO exhibited a series of diffraction peaks with *d*-spacing of 55.5, 26.6, 11.7, 10.8, 9.7, 4.3 and 3.9 Å (Fig. 3b), indicating different structures in the xerogel and precipitate of BOXDH-T12.

To further explore the mechanism for self-assembly, FTIR spectra of BOXDH-T12 xerogel obtained from n-hexanol and precipitates from DMSO were measured, respectively (Fig. 4a and e). The BOXDH-T12 xerogel from n-hexanol exhibited N—H stretching vibrations at 3278 cm^{-1} (the absence of free N—H, a relatively sharp peak with the frequency higher than 3400 cm^{-1}) and amide

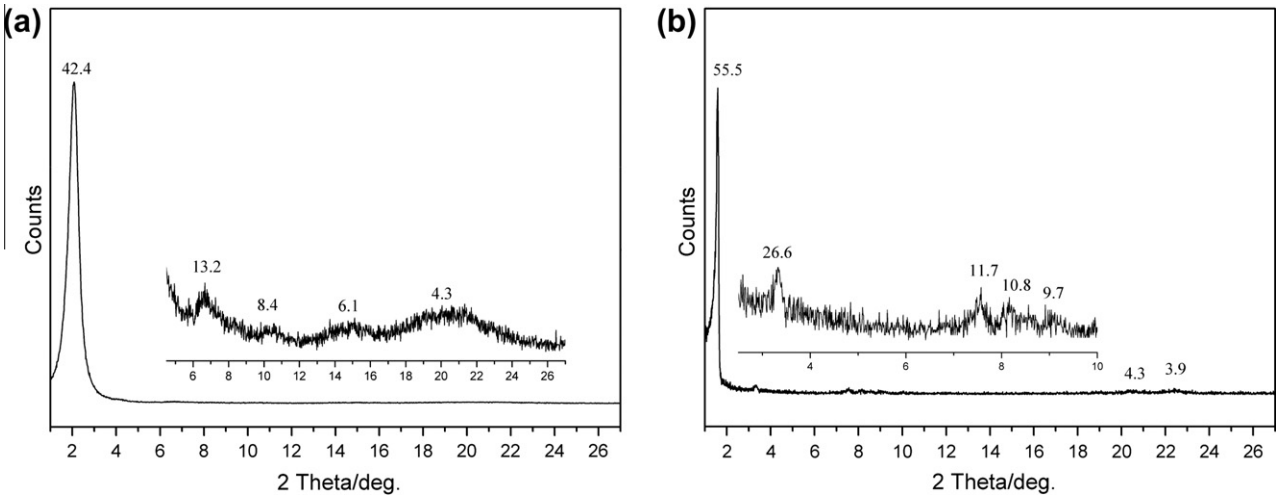

Fig. 3. XRD patterns of (a) BOXDH-T12 xerogel from n-hexanol and (b) precipitate from DMSO.

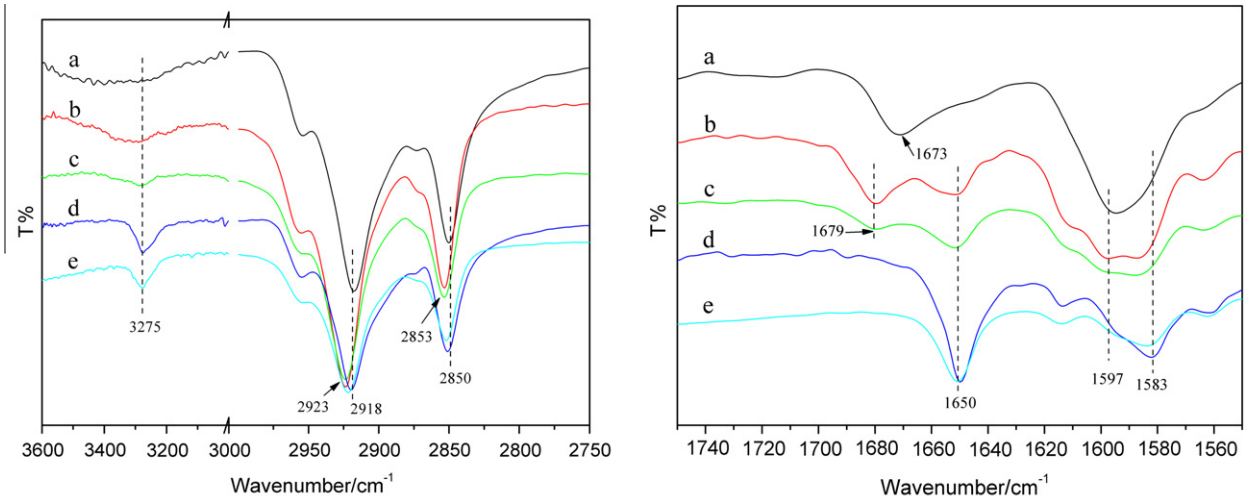

Fig. 4. Partial FTIR spectra of BOXDH-T12 precipitates from (a) DMSO and (d) ethanol and xerogels from DMSO/ethanol with volume ratio of (b) 75:25, (c) 50:50, and (e) n-hexanol.

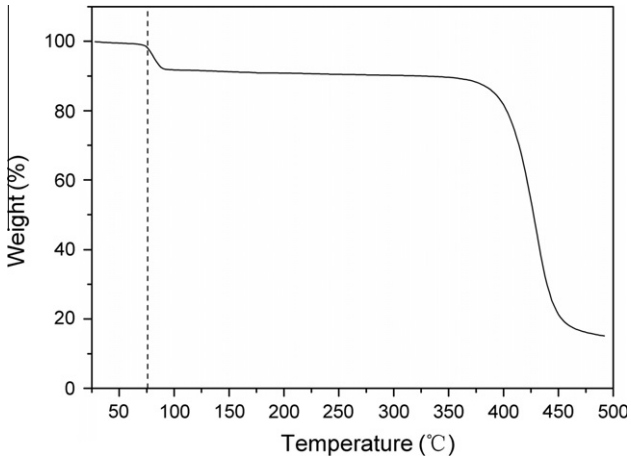

Fig. 5. TGA curve of BOXDH-T12 precipitates from DMSO. A ramp rate of 10 °C/min in nitrogen flow.

I vibration bands at 1651 cm^{-1} (Fig. 4e), indicating hydrogen bonding formation between N—H and C=O groups [20]. In contrast, the BOXDH-T12 precipitates from DMSO showed N—H stretching band centered at 3400 cm^{-1} and amide I band at 1673 cm^{-1} and 1650 cm^{-1} (relatively very weak) (Fig. 4a), suggesting the weak hydrogen bonding interaction. Additionally, the intensity of 1583 cm^{-1} was stronger than 1597 cm^{-1} in the xerogel from n-hexanol, on the contrary, 1597 cm^{-1} was more intense in the precipitates from DMSO, suggesting a considerable dipole-moment change [21]. ^{1}H NMR spectrum of BOXDH-T12 precipitates from DMSO shows a new peak at 2.62 ppm which is assigned to the chemical shift of the CH_3— of DMSO (Fig. S4). The area ratio of the peak at 2.62 ppm to the peak at 4.04 ppm assigned to the —OCH_2— of BOXDH-T12 is one to one, suggesting two equivalents of residual DMSO molecules in the precipitates. Furthermore, the thermal gravimetric analysis (TGA) curve (Fig. 5) shows almost 10% losses of thermograms weight at 75 °C, which corresponds to the weight loss of DMSO and the molar ratio of DMSO/BOXDH-T12 is 2:1 in the precipitates. Based on the results above, we proposed that DMSO molecules might interact with N—H of BOXDH-T12 and induced a slipped aggregation.

Based on above UV–vis, FL, FTIR, TGA and ^{1}H NMR results, two packing modes were depicted in Fig. 6. The strong gelator–gelator hydrogen bonding interactions in alcohols caused the formation of H-aggregate, while the interaction between DMSO molecules and BOXDH-T12 induced the slipped aggregation of BOXDH-T12 in DMSO.

2.3. Gelation properties

The gelation properties of BOXDH-T12 were depended on solvents and its gelling properties in different solvents were summarized in Table 2. BOXDH-T12 was insoluble in the solvents at room temperature, while dissolved to give a clear solution under heating. Upon being cooled to room temperature, it precipitated from DMSO and the short alkyl-chain alcohols and immobile gels formed in the long alkyl-chain alcohols and DMSO/ethanol. The gels were thermoreversible.

It is interesting that BOXDH-T12 can gel the mixtures of DMSO and ethanol although it precipitated from DMSO and ethanol. In the tested mixtures, the CGC of BOXDH-T12 decreased from 2.1×10^{-3} to 1.1×10^{-3} mol/L with the proportion of DMSO/ethanol changing from 80:20 to 50:50 (Table 2), indicating that solvents influenced the gelation of BOXDH-T12. Moreover, BOXDH-T12 precipitated from DMSO consisted of microparticles with diameter of 0.3–2 μm (Fig. S5a) and the precipitates from ethanol showed short fibrillose with width of ca. 0.5 μm (Fig. S5b). In contrast, the xerogels from the mixtures of DMSO/ethanol (75:25) showed slender and straight fibers (Fig. S5c), which packed or fused together to form 3D density network. When volume ratio of DMSO/ethanol changed to 50:50, the xerogel showed both right- and left-handed helical fibers with widths of 0.5–2 μm (Fig. S5d), in some cases, the superhelical ribbons were composed of several helical fibers. The helical structures were also observed by fluorescence microscopy (FM) as shown in Fig. 7a, in which the single ribbons exhibited alternate light and shade fibers with width of approximately 1 μm and the size of light nodes were not uniform. The non-uniform helical pitches and some straight ribbons were also observed, indicating that helical structures were not from a molecular chiral center. Further, the XRD patterns of the xerogels from the mixtures (Fig. S6) differed from that of the precipitates from DMSO (Fig. 3), indicating a different packing structure. The FTIR results that the presence of N—H stretching vibrations at 3250–3400 cm^{-1} and intense absorptions of C=O at 1679 cm^{-1} and 1650 cm^{-1} (Fig. 4b and c) indicated the coexistence of both weak and strong hydrogen bonding in the xerogels from DMSO/

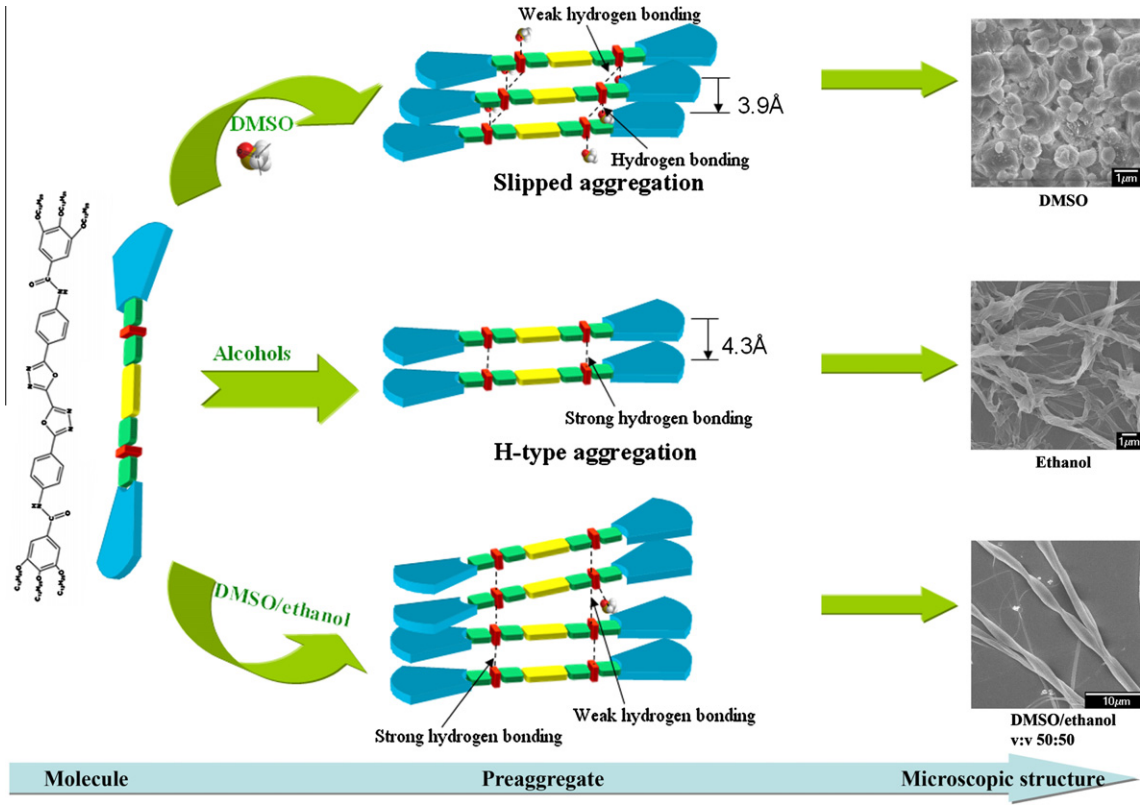

Fig. 6. The schematic representation for the microscopic structure formation of BOXDH-T12 in alcohols, DMSO and DMSO/ethanol.

Table 2
Gelation properties of BOXDH-T12 in mixtures of DMSO/ethanol and primary alcohols.[a].

	BOXDH-T12		BOXDH-T12
DMSO/ethanol(v:v)		Ethanol[b]	P
100:0	P	n-propanol	PG
80:20	*G* (2.1×10^{-3})	n-butanol[c]	*G* (1.2×10^{-3})
75:25	*G* (1.8×10^{-3})	n-pentanol	*G* (6.4×10^{-4})
66:34	*G* (1.4×10^{-3})	n-hexanol	*G* (5.5×10^{-4})
50:50	*G* (1.1×10^{-3})	n-octanol[b]	*G* (6.2×10^{-4})
34:66	P	n-decanol	*G* (6.9×10^{-4})

[a] Concentration: 2.75×10^{-3} mol/L; G, opaque gel; P, precipitates; PG, partly gel formation; Values in bracket denote the critical gelation concentration (mol/L).
[b] Data from the Ref. [17].
[c] Gel is unstable at room temperature.

ethanol. The relative intensity of bands at 1679 cm^{-1} and 1650 cm^{-1} changed with the mixture component. $\nu_{as}(CH_2)$ and $\nu_s(CH_2)$ stretching of BOXDH-T12 in the xerogels shifted to 2923 and 2853 cm^{-1}, which centered at 2918 and 2850 cm^{-1} in the precipitates from DMSO (Fig. 4a) and ethanol (Fig. 4d), indicating weaker van der Waals interaction and less ordered alkyl chains in the xerogels. Thus, the helical fibers might be induced by the different H-bonding as shown in Fig. 6. However, the exact mechanism for the helical fiber formation of BOXDH-T12 in the mixtures is unclear at this stage.

On the other hand, BOXDH-T12 could form stable gel in long alkyl-chain alcohols, such as n-butanol, n-pentanol, n-hexanol, n-octanol [17] and n-decanol with CGC of 6.4×10^{-4}, 5.5×10^{-4}, 6.2×10^{-4} and 6.9×10^{-4} mol/L, respectively, suggesting that it is a supergelator in alcohols. The xerogel from n-hexanol as well as the xerogels from other alcohols was composed of entangled 3D fibrillar network as shown in Fig. 7b. Although it was found that the gel formation time of BOXDH-T12 in these alcohols decreased exponentially with an increase of gelator concentration (Fig. S7), the gel formation time strongly depended on the solvents. For

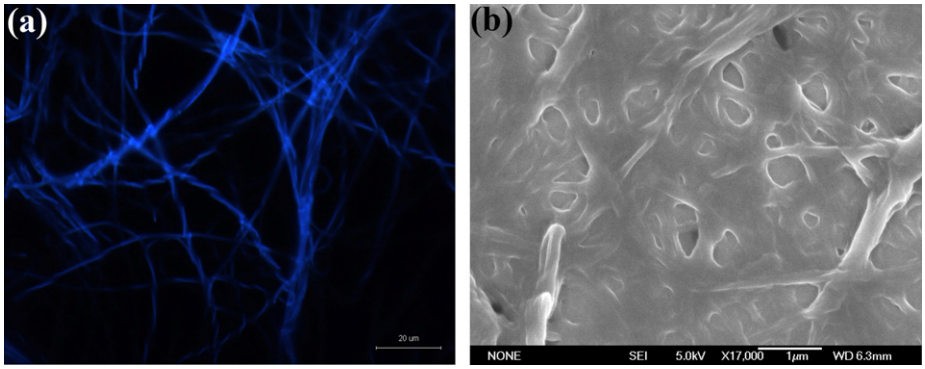

Fig. 7. (a) Fluorescence microscopic photo of BOXDH-T12 xerogel from DMSO/ethanol (50:50) and SEM images of the xerogels from (b) n-hexanol (7×10^{-4} mol/L).

the studied gelator, the gel formation time increases in the order of n-pentanol gel < n-hexanol gel < n-octanol gel < n-decanol gel as shown in Fig. S8. This might be attributed to the stronger solvophobic interactions (weaker interactions between solvents and alkoxyl chains of gelator) and thus lower tendency of BOXDH-T12 to crystallize in longer alkyl-chain alcohol. FTIR spectra of the xerogels and corresponding gels show the N—H stretching vibration and amide I vibration bands at 3279 and 1651 cm^{-1} (Fig. S9), respectively, which indicate that the alcohol molecules slightly affected the gelator–gelator hydrogen bonding. However, BOXDH-T12 precipitated from the short alkyl-chain alcohols (ethanol) showed the $\nu_{as}(CH_2)$ and $\nu_s(CH_2)$ stretching at 2918 and 2850 cm^{-1} (Fig. 4d), indicating that the solvophobic/solvophilic effect influenced the gelling behaviors of BOXDH-T12.

3. Conclusion

BOXDH-T12 showed a monomeric feature and intramolecular charge transition at concentrations lower than 1×10–5 mol/L. UV–vis and FL spectra of BOXDH-T12 and indicated that H-aggregates formed in alcohols and slipped packing aggregates in DMSO. FTIR, 1H NMR, WAXD and TGA results of BOXDH-T12 precipitates and xerogels suggest that the interaction between DMSO and BOXDH-T12 molecules caused BOXDH-T12 slipped stacking in DMSO and induced helical fiber formation in DMSO/ethanol. BOXDH-T12 can gel the mixtures of DMSO and ethanol and long alkyl-chain alcohols due to a balance of hydrogen bonding, π–π stacking and van der Waals interactions. Solvophobic/solvophilic effect influenced the gelling behaviors of BOXDH-T12 in alcohols.

4. Experimental section

Experimental details: BOXDH-T12 was prepared following our previously work. Fourier transform infrared (FTIR) spectra were recorded with a Perkin–Elmer spectrometer (Spectrum One B). The FTIR spectra of the xerogel and precipitate samples were measured on silicon wafer. Photoluminescence was measured by a Perkin–Elmer LS 55 spectrometer and the absorption measurements were used a UV-2550 spectrometer. ^{1}H NMR spectra were recorded with Varian-Unity 500 MHz spectrometer, using tetramethylsilane (TMS) as an internal standard. Thermogravimetric analysis (TGA) curve was measured by SDTQ600. SEM observations were taken with a JSM-6700F apparatus. Fluorescence microscopy (FM) images were carried out with an Olympus BX51TRF microscope. The light source for fluorescence microscopy observation was a mercury lump with a fluorescent filter cube, which provides excitation in the range of 330–385 nm, and collects the emission at >420 nm. Intensity of the fluorescence emission was measured using the built-in CCD camera along with the associated software. The samples for SEM and FM measurement were prepared by dropping a small amount of gel on a silicon and glass wafer respectively, then by lyophilization. X-ray diffraction was carried out with a Bruker Avance D8 X-ray diffractometer.

Acknowledgements

The authors are grateful to the National Science Foundation Committee of China (Project Nos. 51073071, 51103057, 21072076), and Project 985-Automotive Engineering of Jilin University for their financial support of this work.

Appendix A. Supplementary material

Supplementary data associated with this article can be found, in the online version, at http://dx.doi.org/10.1016/j.molstruc.2012.12.037.

References

[1] M.F.J. Hoeben, P. Jonkheijm, E.W. Meijer, A.P.H. Schenning, Chem. Rev. 105 (2005) 1491–1546.
[2] (a) C.W. Struijk, A.B. Sieval, J.E.J. Dakhorst, M. van Dijk, P. Kimkes, R.B.M. Koehorst, H. Donker, T.J. Schaafsma, S.J. Picken, A.M. van de Craats, J.M. Warman, H. Zuilhof, E.J.R. Sudholter, J. Am. Chem. Soc. 122 (2000) 11057–11066;
(b) X.-Q. Li, V. Stepanenko, Z. Chen, P. Prins, L.D.A. Siebbeles, F. WGrthner, Chem. Commun. (2006) 3871–3873;
(c) Y. Che, A. Datar, K. Balakrishnan, L. Zang, J. Am. Chem. Soc. 129 (2007) 7234–7235;
(d) Y.-L. Yu, H.-Y. Du, J.-H. Zhang, J. Mol. Struct. 1005 (2011) 107–112.
[3] (a) G.H. Brown, J.J. Wolken, Liquid Crystals and Biological Structures, Academic Press, New York (USA), 1979;
(b) G.M. Whitesides, B. Grzybowski, Science 295 (2002) 2418;
(c) H. Ringsdorf, B. Schlarb, J. Venzmer, Angew. Chem. Int. Ed. Engl. 27 (1988) 113;
(d) M.daG. Miguel, H.D. Burrows, S.J. Formosinho, B. Lindman, J. Mol. Struct. 563–564 (2001) 89–98.
[4] (a) F.M. Hoeben, P. Jonkheijm, E.W. Meijer, A.P.H.J. Schenning, Chem. Rev. 105 (2005) 1491;
(b)F. Würthner (Ed.), Supramolecular Dye Chemistry, Topics in Current Chemistry, vol. 258, Springer, Berlin (Germany), 2005;
(c) E. Westphal, I.H. Bechtold, H. Gallardo, Macromolecules 43 (2010) 1319–1328;
(d) J. Tang, R. Huang, H. Gao, X. Cheng, M. Prehm, C. Tschierske, RSC Adv. 2 (2012) 2842–2847.
[5] (a) V. Percec, C.-H. Ahn, T.K. Bera, G. Ungar, D.J.P. Yeardley, Chem. Eur. J. 5 (1999) 1070;
(b) V. Percec, M.R. Imam, T.K. Bera, V.S.K. Balagurusamy, M. Peterca, P.A. Heiney, Angew. Chem. Int. Ed. 44 (2005) 4739;
(c) Y. Sagara, S. Yamane, T. Mutai, K. Araki, T. Kato, Adv. Funct. Mater. 19 (2009) 1869;
(d) A. Das, S. Ghosh, Chem. Eur. J. 16 (2010) 13622.
[6] T.-E. Kaiser, H. Wang, V. Stepanenko, F. Würthner, Angew. Chem. Int. Ed. 46 (2007) 5541–5544.
[7] H. Maeda, Y. Terashima, Chem. Commun. 47 (2011) 7620–7622.
[8] Y. Chen, Y. Lv, Y. Han, B. Zhu, F. Zhang, Z. Bo, C.-Y. Liu, Langmuir 25 (2009) 548–8555.
[9] S. Yagai, T. Seki, T. Karatsu, A. Kitamura, F. Würthner, Angew. Chem. Int. Ed. 47 (2008) 3367–3371.
[10] (a)F. Fages (Ed.), Low Molecular Mass Gelators, Topics in Current Chemistry, Springer, Verlag, Berlin, 2005;
(b)T. Ishi-I, S. Shinkai, F. Würthner (Eds.), Supramolecular Dye Chemistry in Topics in Current Chemistry, Springer, Verlag, Berlin, 2005, p. 119;
(c)R.G. Weiss, P. Terech (Eds.), Molecular Gels, Springer, Dordrecht, 2006.
[11] A. Pal, J. Dey, Langmuir 27 (2001) 3401–3408.
[12] S.Y. Ryu, S. Kim, J. Seo, Y.-W. Kim, O.-H. Kwon, D.-J. Jang, S.Y. Park, Chem. Commun. (2004) 70–71.
[13] I. Furman, R.G. Weiss, Langmuir 9 (1993) 2084–2088.
[14] J. Cui, A. Liu, Y. Guan, J. Zheng, Z. Shen, X. Wan, Langmuir 26 (2010) 3615–3622.
[15] P. Zhu, X. Yan, Y. Su, Y. Yang, J. Li, Chem. Eur. J. 16 (2010) 3176–3183.
[16] S. Qu, L. Zhao, Z. Yu, Z. Xiu, C. Zhao, P. Zhang, B. Long, M. Li, Langmuir 25 (2009) 1713–1717.
[17] The synthesis of BOXDH-T12 has been reported in our previous paper named "Gel ability and fluorescence-enhanced emission of a new bi-1,3,4-oxadiazole derivative" which was accepted by soft materials but not published. http://dx.doi.org/10.1080/1539445X.2011.633147.
[18] (a) R. metivier, R. Amengual, I. Leray, V. Michelet, J.-P. Genet, Org. Lett. (2004) 739;
(b) A. Miyazaki, T. Enoki, New J. Chem. 33 (2009) 1249–1254.
[19] (a) J.M. Kroon, R.B.M. Koehorst, M. van Dijk, G.M. Sanders, E.J.R. Sudho Lter, J. Mater. Chem. 7 (1997) 615;
(b) R. Rubires, J. Crusats, Z. El-Hachemi, T. Jaramillo, M. López, E. Valls, J.-A. Farrera, J.M. Ribó, New J. Chem. (1999) 189–198.
[20] P.I. Harris, D. Chapman, Biopolymers 37 (1995) 251–263.
[21] L. J. Bellamy (Ed.), The Infra-red Spectra of Complex Molecules, third ed., Chapman and Hall Ltd, 1975.